Hexagonal heterolayers on a square lattice: A combined STM and LEED study of FeO(111) on Pt(100)

Sh. Shaikhutdinov,* M. Ritter, and W. Weiss
Fritz-Haber-Institut der Max-Planck-Gesellschaft, Faradayweg 4-6, Berlin 14195, Germany
(Received 17 March 2000)

Formation of an epitaxial iron oxide monolayer on a Pt(100)-hex substrate was studied by scanning tunneling microscopy (STM) and low-energy electron diffraction (LEED). High-resolution STM images reveal a sinusoidal height modulation of the top atomic rows along the [011] direction of the original Pt(100)-hex substrate. This modulation is assigned to the buckling of the top oxygen layer due to the interaction with Pt substrate atoms. Two superstructures, described as FeO(111)/Pt(100)-$c(2\times10)$ and (2×9) coincidence structures, coexist on the surface. The latter structure results in a much lower Pendry R factor in dynamical LEED analysis than earlier reported for a $c(2\times10)$ structure. Numerous islands with the same surface structure as the terraces develop on the dense FeO overlayer. They are assigned as the Pt(100)-(1×1) islands formed during the hex$\rightarrow(1\times1)$ reconstruction of the Pt substrate underneath the FeO(111) bilayer. The islands are rectangular and elongated in the direction of hex reconstruction on the original Pt(100). Combined STM and LEED data clearly indicate that anisotropy in the substrate reconstruction leads to anisotropy of the oxide overlayer.

I. INTRODUCTION

Heteroepitaxy is a versatile route to produce clean and well-ordered metal oxides with defined stoichiometry. For example, thin films of iron, zirconium, chromium, and titanium oxides have been prepared on platinum substrates,[1–4] by evaporating the metal onto a clean substrate and then oxidizing at 800–1000 K in $\sim10^{-6}$ mbar of oxygen gas pressure. These films can be used as well-defined model systems for investigation of the catalytic, magnetic, etc. properties of oxides as recently demonstrated with iron oxide films.[5]

The structure and chemical properties of iron overlayers on platinum surfaces were studied by Vurens *et al.*[1] A coincidence structure of a hexagonal FeO(111) layer on a hexagonal Pt(111) substrate was suggested in order to explain the characteristic satellites around the substrate integral spots in the corresponding low-energy electron diffraction (LEED) patterns. Photoelectron diffraction measurements revealed that the iron oxide overlayer consists of an Fe-O bilayer with oxygen on top. The iron-oxygen interlayer distance was found to be highly compressed by about 50% relative to bulk FeO.[6] In scanning tunneling microscopy (STM) images, a hexagonal superstructure with $\sim$26 Å periodicity was observed. The STM images were explained by Galloway, Benitez, and Salmeron as a $\begin{pmatrix}9 & 1\\ -1 & 10\end{pmatrix}$ coincidence structure of a FeO(111) bilayer on Pt(111).[7] Later, Ritter, Over, and Weiss found slightly different coincidence structures using STM and spot-profile analysis LEED techniques.[8]

With the Pt(100) substrate, one can expect other iron oxide structures to form. The clean Pt(100) surface is characterized by a quasihexagonal layer resting on top of the square (1×1) lattice. Because the two lattices are incommensurate, large periodic structures are formed on the surface, such as Pt(100)-(5×20) and Pt(100)-$\begin{pmatrix}N & 1\\ -1 & 5\end{pmatrix}$, where $N=12-14$, which are also referred to as Pt(100)-hex and Pt(100)-hex-$R0.7°$, respectively. However, a dynamical LEED analysis of the FeO/Pt(100) interface showed again that the quasihexagonal FeO(111) bilayer with oxygen on top grew on the square Pt(100)-(1×1) surface, resulting in an FeO(111)/Pt(100)-$c(2\times10)$ coincidence structure.[9]

Several STM studies have recently been reported of homo- and heteroepitaxial growth of metal on hex reconstructed surfaces, for example, Pt on Pt(100)-hex,[10] Au on Pt(100)-hex-$R0.7°$,[11] and Fe on Au(100)-hex.[12] The STM results indicate that the anisotropy in the substrate surface reconstruction leads to anisotropy of the metal overlayer. To our knowledge, no STM studies have yet been performed on oxide overlayers grown on the hex-reconstructed substrates.

In this paper, we present a STM study of the FeO(111) overlayer grown on a Pt(100) substrate. We focus on investigation of the FeO overlayer at monolayer coverage, where STM and dynamical LEED analysis provide complementary information. STM images reveal a characteristic height modulation of the atomic rows in the {011} direction, which we assign to the buckling of the top oxygen atoms due to their interaction with the Pt substrate. Two superstructures described as a FeO(111)-Pt(100)-$c(2\times10)$ and a (2×9) coincidence structure coexist on the surface. The latter structure is characterized by a much lower Pendry R factor in LEED analysis than that of a $c(2\times10)$ structure previously reported.[8]

II. EXPERIMENT

The experiments were performed in an UHV chamber (a base pressure below 1×10^{-10} mbar) equipped with STM, back-view LEED, Auger electron spectroscopy (AES), and standard facilities for sample cleaning.[13] The Pt(100) single-crystal surface was cleaned by repeated cycles of ion sputtering and annealing to 1300 K until no contamination was detected by AES and the LEED pattern exhibited sharp spots corresponding to the Pt(100)-hex structure. Iron (5.0, Aldrich Chemicals) was deposited at a rate of $\sim$0.1 monolayers (ML) per min using an electron-beam-assisted evaporator (Omicron) onto a Pt substrate kept at room temperature. During the evaporation the pressure did not exceed 1×10^{-9} mbar. Subsequently, the sample was oxidized at 730–800 K in

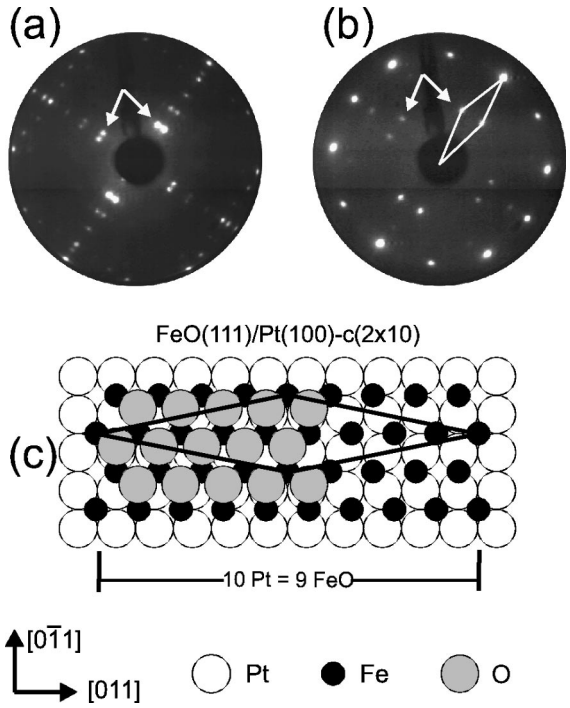

FIG. 1. LEED patterns of the Pt(100)-hex (a) and the FeO(111)/Pt(100) (b) surfaces at electron energy $E=50$ eV. The arrows indicate the spots coming from two orthogonal domains. (c) Top view of the model illustrating an FeO(111)/Pt(100)-$c(2\times10)$ coincidence structure. For clarity, not all top atoms are drawn.

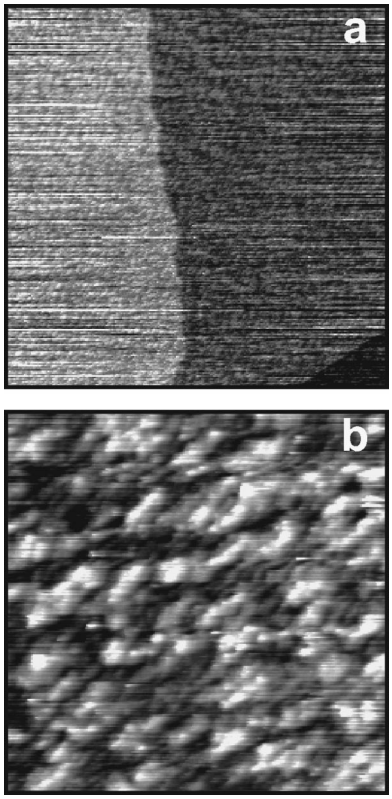

FIG. 2. 5000×5000 Å^2 (a) and 750×750 Å^2 (b) STM images of the Pt(100) surface after deposition of ~1 ML of metallic iron. The surface is roughened with an average corrugation of ~1.5 Å, as shown in (b). Monatomic steps of the original Pt substrate are visible in image (a).

10^{-6} mbar oxygen for ~5–30 min until the LEED pattern showed bright diffraction spots corresponding to a coincidence superstructure. AES spectra of the samples studied showed only signals from Pt, Fe, and O atoms.

For the dynamical LEED analysis, diffraction patterns in the 40–300 eV electron beam energy range were collected using video camera connected to a computer. The I-V measurements were performed at ~120 K. The curve analysis was performed using the symmetrized automated tensor LEED software package.[14]

The STM images presented in this paper were obtained at tunneling voltages of ~30–200 mV applied to the sample and a current of ~1.5 nA. The tungsten tip was electrochemically etched and subsequently annealed in UHV by electron-beam heating. The characteristic STM images were independent of bias polarity and applied voltage.

III. RESULTS

A. Preparation of FeO monolayer on Pt(100)

Figure 1(a) shows a LEED pattern of the clean, hex-reconstructed Pt(100) surface. The LEED pattern exhibits diffraction spots coming from the two orthogonal domains, as marked by the arrows, present on the surface with different weight factors. The corresponding STM images (not presented here for conciseness) show ~1000-Å-wide terraces separated by monatomic steps of ~2 Å, corresponding to the interlayer distance of Pt(100). During Fe deposition onto this surface, the ''hex'' spots in the LEED patterns gradually vanished, and only the diffuse spots of the Pt(100)-(1×1) surface remained at an Fe coverage of about 1 ML, as determined from the Pt(237 eV) to Fe(652 eV) intensity ratio in the corresponding AES spectra.[9] At this point, the STM images in Fig. 2 show that the originally flat terraces become rough with a corrugation amplitude of about 1.5 Å. However, some preferential direction of islandlike species on the surface can be seen in Fig. 2(b).

Oxidation in 10^{-6} mbar O_2 at ~800 K results in the LEED pattern shown in Fig. 1(b), which has been attributed previously to an FeO(111)/Pt(100)-$c(2\times10)$ coincidence structure. At low FeO coverage, the pattern is superimposed on that of the original Pt(100)-hex surface, with a weight factor depending on the amount of predeposited iron. This implies that the iron oxide phase grows via domains surrounded by the reconstructed Pt(100)-hex surface. Therefore the formation of a dense FeO overlayer can be ascertained by the disappearance of the diffraction spots corresponding to the Pt(100)-hex surface. These FeO/Pt(100) surfaces have been investigated by both STM and LEED, and are discussed in the following sections.

It should be mentioned that the oxidation procedure used with the Pt(100) substrate (~750 K, 20–30 min) differs from that used for the preparation of an FeO monolayer on the Pt(111) substrate (~1000 K, 2 min).[8] The latter procedure results in a film of poor quality as judged by STM. The high-temperature oxidation probably causes a partial dissolution of the overlayer into the Pt substrate, as was observed by ion-surface scattering experiments.[1] This effect can be more pronounced on the more open Pt(100) surface than on the close-packed Pt(111) surface.

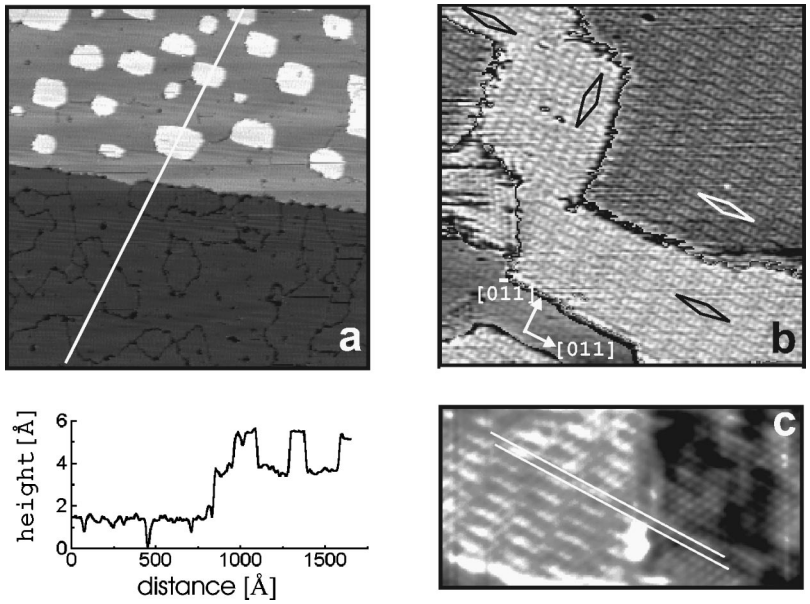

FIG. 3. (a) $1500\times1500\,\text{Å}^2$ STM image of a dense FeO(111) layer on Pt(100). Numerous islands are formed in the upper terrace. The lower terrace represents an uncommon area free of any islands with clearly defined domain boundaries. Both the step height separating the two terraces and that of the islands are equal to 2 Å, corresponding to one interlayer distance in Pt(100), as measured by the profile line shown below image (a). (b) $105\times105\,\text{Å}^2$ STM image of FeO(111) on Pt(100) presented with differentiated contrast in order to show the identical surface structure on both terrace and islands. Three domains coalesce: the central one is orthogonal to two adjacent ones as indicated by the unit cells. The islands are near rectangular and always elongated in the [011] direction with the aspect ratio depending on preparation. On the corner of the domain in the left part of the image is a region exhibiting a hexagonal lattice of protrusions. (c) $70\times35\,\text{Å}^2$ STM image showing two neighboring domains, exhibiting a characteristic modulation of the FeO surface (on the left) and hexagonal lattice of protrusions (on the right). The atomic row of protrusions on the FeO surface is aligned with one of the three close-packed directions of the hex structure and lies between the atomic rows indicated by lines.

B. STM study of FeO monolayer on Pt(100)

Figure 3(a) shows a $1500\times1500\,\text{Å}^2$ STM image of the FeO overlayer on Pt(100) at a monolayer coverage. The step height of ~2 Å separating adjacent terraces in this image results from the substrate morphology. The height of islands seen on the upper terrace is also found to be ~2 Å, as shown by the profile line below the image (a). The islands are nearly rectangular in shape and slightly elongated in the direction parallel to the step edge. The aspect ratio (length/width) varies between 1 and 3 depending on the preparation. The islands are randomly distributed on the surface. However, regions that are free of islands are occasionally observed, with the boundaries between the neighboring domains clearly seen as depressed lines [see bottom of Fig. 3(a)]. The boundaries develop between domains with orthogonal orientation but also between domains of the same orientation, as evidenced by high-resolution STM images.

Both terraces and islands exhibit an identical surface superstructure. The parameter of the unit cell indicated in Fig. 3(b) is larger in one of the {011} directions depending on the domain orientation, which is henceforth referred to as the direction of overlayer reconstruction. Figure 3(b) shows a region of coalescence between three islands, where the structure of the central island is orthogonal to the two adjacent ones. The islands are always found elongated in the direction of the reconstruction.

Figure 4 shows high-resolution STM images of the FeO/Pt(100) surface. A sine-wave height modulation of the atomic rows in the [011] direction is clearly seen on the profile line *A* below the image (a). Given the Pt(100) lattice constant of 2.77 Å, the averaged periodicity lengths, measured by STM, of ~5.5 and ~25 Å in two perpendicular {011} directions can be described as the $(2\times N)$ superstructure, where $N\sim9-10$. Unfortunately, an atom position cannot be precisely determined because the ''negative'' part of the modulation wave is cancelled by the protrusions in the ''positive'' part of two neighboring waves. When the adjacent waves interfere, a characteristic zigzag line is observed running perpendicular to the direction of reconstruction as marked by the arrow in Fig. 4(a). Assuming that this image manifests a $c(2\times10)$ coincidence structure as depicted in Fig. 1(c), it is possible to assign the atom positions and corresponding unit cell as indicated in Fig. 4(a).

The two-dimensional fast Fourier transform (FFT) map of the STM image in Fig. 4(a) is shown below together with the corresponding LEED pattern. One can see a close similarity between FFT and LEED. The FFT map clearly shows a hexagonal symmetry of the top layer and a long-range surface periodicity, which occur due to the height modulation of atomic rows.

However, a close inspection of high-resolution STM images reveals many regions that exhibit a (2×9) superstructure as shown in Fig. 4(b). No domain boundaries between $c(2\times10)$ and (2×9) structures have been observed by STM, otherwise it would be possible to estimate the relative coverage of each structure from the large-scale images. STM observation of the (2×9) coincidence structure inspired us to reinvestigate a dynamical LEED analysis of the same surface.

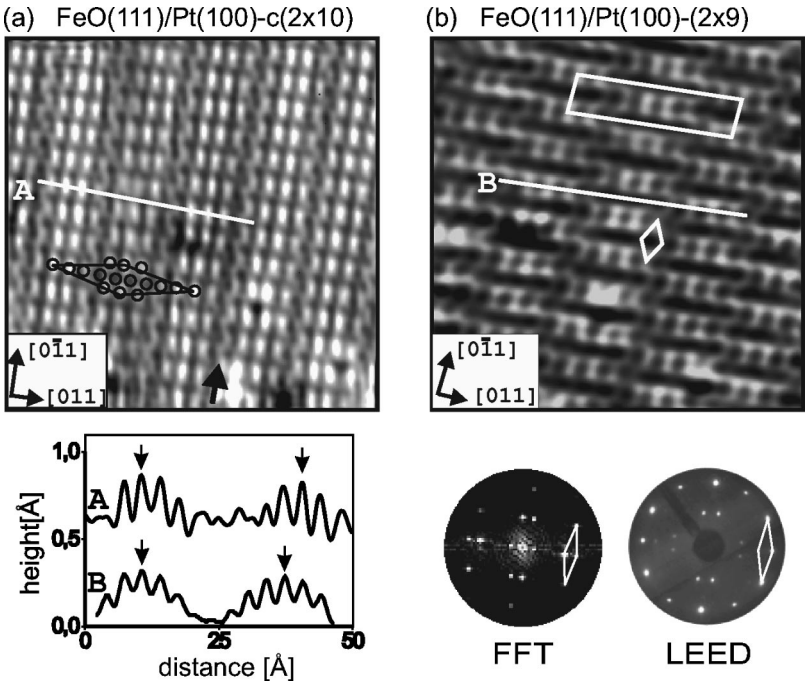

FIG. 4. High-resolution $70\times70\,\text{Å}^2$ (a) and $55\times55\,\text{Å}^2$ (b) STM images of a FeO(111) monolayer on Pt(100). Profile lines *A* and *B* shown below image (a) reveal a sinusoidal height modulation of atomic rows along the [011] direction. The atom positions deduced within a $c(2\times10)$ coincidence cell are shown on the image (a) by circles. Arrow on image (a) shows a characteristic zigzag line running along the $[0\bar{1}1]$ direction, which is produced when two adjacent modulation waves interfere. Image (b) shows the region exhibiting a (2×9) coincidence structure. A FFT map of the image (a) is shown together with the corresponding LEED pattern.

C. LEED analysis of FeO monolayer on Pt(100)

In order to focus on a single domain orientation, diffraction spots coming from the orthogonal domain were covered by black dots in the LEED pattern, as shown in Fig. 5(a). In the schematic representation in Fig. 5(b) the crosses indicate the substrate spot positions, and the large dots the FeO(111)-(1×1) spot positions. The FeO($\bar{n}n$) and Pt($0n$) spots coincide. Weak spots, which can result from multiple-scattering events between the FeO overlayer and Pt substrate, are indicated by small dots. The latter can be described by the following scattering vector sums: spot 1 near the (00) beam by $\mathbf{g}(21)_{\text{Pt}}+\mathbf{g}(0\bar{2})_{\text{FeO}}$, spot 2 by $\mathbf{g}(10)_{\text{Pt}}+\mathbf{g}(\bar{1}0)_{\text{FeO}}$, spot 3 by $\mathbf{g}(20)_{\text{Pt}}+\mathbf{g}(\bar{2}0)_{\text{FeO}}$, spot 4 by $\mathbf{g}(\bar{2}\,1)_{\text{Pt}}+\mathbf{g}(03)_{\text{FeO}}$, spot 5 by $\mathbf{g}(20)_{\text{Pt}}+\mathbf{g}(\bar{1}0)_{\text{FeO}}$, spot 6 by $\mathbf{g}(1\,\bar{1})_{\text{Pt}}+\mathbf{g}(02)_{\text{FeO}}$, and spot 7 by $\mathbf{g}(3\bar{1})_{\text{Pt}}+\mathbf{g}(\bar{2}0)_{\text{FeO}}$. Spot 1 is hidden by the electron gun in Fig. 5(a); and spots 6 and 7 are too weak to be visible in this pattern, but show up at other energies.

As mentioned above, this LEED pattern has been previously attributed to a $c(2\times10)$ coincidence structure of a quasihexagonal Fe-O bilayer on the Pt(100)-(1×1) surface.[1,9] However, based on the STM observation of an additional (2×9) superstructure, we performed a best-fit search assuming the FeO(111)/Pt(100)-(2×9) structure depicted in Fig. 5(c). Again, a slightly distorted hexagonal FeO(111) bilayer with oxygen on top is assumed, with Fe and O atom rows being aligned to the Pt atom rows in the [011] direction.

In the first iteration, the platinum-iron and iron-oxygen interlayer distances were varied from 1.0 to 2.3 Å and from 0.0 to 1.3 Å, respectively. A minimum *R* factor was obtained with 2.2 and 0.6 Å for the Pt-Fe and Fe-O interlayer distances, respectively. Then the registry of the FeO bilayer with respect to the substrate was varied in steps of 0.1 Å along the $[0\bar{1}1]$ direction. The *R* factor of 0.20 was reached with ~0.2 Å lateral shift of the overlayer in the $[0\bar{1}1]$ direction. Any shift of the oxygen atoms from the threefold hollow sites on the Fe sublayer increased the *R* factor.

Subsequently, slight deviations of atoms within the iron and oxygen layers were tested. At first, the Fe atoms were sinusoidally displaced in a vertical direction, while the O layer was kept either planar with a regular lateral arrangement of the atoms, or buckled with all Fe-O interatomic distances alike. This produced no significant improvement of the *R* factor. Then the vertical position of every single atom was varied in steps of 0.1 Å. Out-of-plane deviations were kept if they resulted in an improved fit.

The best fit is characterized by an *R* factor of 0.15 (±0.02). The comparison between the calculated and experimental *I-V* curves is shown in Fig. 6. The *R* factor is much lower than that of 0.40 (±0.02) for the previously reported[9] $c(2\times10)$ reference structure. However, our search resulted in two distinct structures with the same *R* factor. The structures differ in the lateral coordinates of Fe atoms and both the lateral and vertical coordinates of O atoms. We reported similar uncertainty in our previous paper,[9] where three structures within the same $c(2\times10)$ model resulted in identical *R* factors. It seems plausible that convergence to a single structure is obviated by the coexistence of the $c(2\times10)$ and $p(2\times9)$ structures, as observed in the present STM study.

Nevertheless, we have calculated the mean interlayer and Fe-O and Pt-Fe next-neighbor distances and the registries as presented in Table I. The ion radii can be estimated using a hard-sphere approximation. Starting from the atomic radius of the platinum atoms of 1.39 Å, we have found the radii of 1.27 and 0.66 Å for the Fe and O ions, respectively. These values are used for presentation of the model depicted in Fig. 5(c).

IV. DISCUSSION

Iron deposition at monolayer coverage depletes the hex reconstruction of the Pt(100) surface since only diffuse

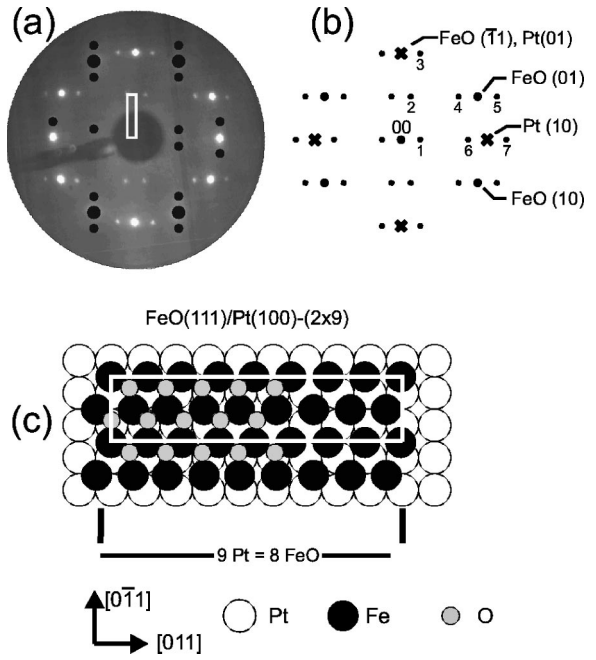

FIG. 5. (a) LEED pattern of ~1 ML FeO overlayer on Pt(100) at $E=90$ eV where diffraction spots coming from one of the orthogonal domains are covered by black dots in order to focus on a single domain orientation. A (2×9) coincidence unit cell is indicated. (b) Schematic representation of pattern (a) where the crosses indicate substrate spot positions, and the large dots the FeO(111)-(1×1) spot positions. The FeO($\bar{n}n$) and Pt($0n$) spots coincide. The weak spots, which can result from multiple-scattering events between FeO overlayer and Pt substrate, are indicated by the small dots. (c) Top view of the model of slightly distorted oxygen-terminated FeO(111) bilayer surface represented with the relative radii determined from the best-fit structure data presented in Table I below. For clarity, not all top atoms are drawn.

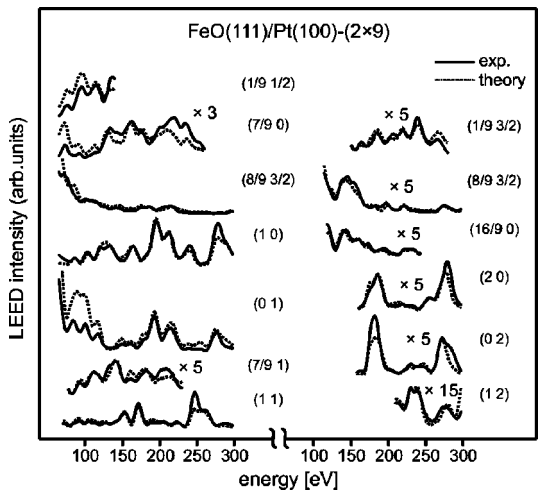

FIG. 6. Comparison of the experimental and simulated I-V curves for the best-fit structure obtained on the FeO(111)/Pt(100)-(2×9) surface. The data set covers a total energy range of 2200 eV. The best fit has a Pendry R factor of 0.15 (±0.02).

Pt(100)-(1×1) spots are observed in the LEED pattern. The Volmer-Weber mode has been suggested for the growth of iron on Pt(111), where three-dimensional Fe particles start to grow from the beginning.[15] With the Pt(100) substrate, however, one should consider that the hex surface accommodates about 25% more Pt atoms than the (1×1) surface. At room temperature, the hex$\rightarrow(1\times1)$ surface reconstruction can form islands of excess Pt atoms as evidenced by *in situ* STM measurements of the Pt(100)-hex-$R0.7°$ surface during CO and O_2 adsorption.[16] Therefore, the roughening of the surface obtained after iron deposition in Fig. 2 can also be attributed to a mixture of both Fe and Pt islands. Similar behavior has been observed on the Fe/Au(100)-hex surface at an Fe coverage of more than 0.5 ML.[12]

Exposure of the Fe/Pt(100) surface to 10^{-6} mbar of oxygen at elevated temperatures results in oxidation of the iron overlayer and formation of the well-ordered FeO(111) surface on top of the Pt(100)-(1×1) substrate as judged by LEED. STM images of the FeO(111)/Pt(100) surface reveal a characteristic height modulation of ~0.3 Å amplitude of the atomic rows along the [011] direction (Fig. 4). This modulation is very similar to those found for the hex-reconstructed Pt(100) and Au(100) surfaces.[10–12,16,17] For the Pt(100)-hex surface, helium atom scattering measurements[18] revealed the buckling of the top layer by about 0.5 Å, which is nearly identical to the value measured by STM.[10] Taking into account the close similarity between the FFT map and the LEED pattern, both shown in Fig. 4, our data strongly indicate that the buckling of the surface observed by STM for the FeO(111)/Pt(100) system has a topographic origin, which means that the FeO overlayer atoms are displaced normal to the substrate surface.

This kind of surface modulation seems to be intrinsic for systems where the hexagonal top layer rests on a square (100) lattice. However, in contrast to the Pt(100)-hex surface, the FeO(111)/Pt(100) interface stacks into the bulk as O_{hex}-Fe_{hex}-$Pt_{square(1)}$-$Pt_{square(2)}$ . . . layers, i.e., as *two* hex layers on top of a square-lattice substrate, as evidenced by the present LEED analysis. In other words, the substrate square lattice is located in the third sublayer and hence might not drastically influence the topography of the top hexagonal layer. This indicates some specific interaction of the FeO layer with the Pt(100) substrate.

In the corner of the island visible in the left part of Fig. 3(b) and in another STM image in Fig. 3(c), one can see areas exhibiting a hexagonal lattice of protrusions. Such small regions cannot affect our LEED analysis indicating an O termination of the FeO(111) surface. The hex structure appears about 0.3–0.5 Å lower than the modulated FeO surface. This distance is close to the Fe-O interlayer distance (~0.65 Å) obtained for the best fit in the LEED analysis (see Table I). In addition, the modulated atomic rows on the FeO surface are aligned with one of the three close-packed directions of the hex structure and lie between atomic rows thereof, as marked in Fig. 3(c). This fits well the model of an FeO(111) bilayer terminated by oxygen, if the protrusions on the hex structure correspond to the Fe atoms and the protrusions on the modulated FeO surface are attributed to the O atoms in the top layer.

The last assignment is in line with theoretical calculations of the origin of contrast in STM images of FeO(111)/Pt(111) surface performed by Galloway, Sautet, and Salmeron using electron-scattering quantum chemistry theory.[19] They found that the protrusions in corresponding STM images must be

TABLE I. The average values (Å) of the interlayer distances, the registry shifts, and the next-neighbor distances in the FeO(111)/Pt(100)-(2×9) interface as found by dynamical LEED analysis.

Interlayer distance		Registry shift in $[0\bar{1}1]$		Next-neighbor distance	
Pt-Fe	Fe-O	Fe	O	Pt-Fe	Fe-O
2.20	0.64	0.15	0.25	2.66	1.93

always due to the surface O atoms. We believe that this conclusion is valid for the Pt(100) substrate as well, since the calculation investigated all mutual orientations of Fe and O with respect to the Pt substrate.

Interestingly, a characteristic modulated structure is observed on the hexagonal FeO/Pt(100) surface but not on the hexagonal Fe/Pt(100) surface. This indicates that a long-range modulation of the FeO surface is induced by the interaction of the top oxygen layer with a Pt substrate, resulting in out-of-plane displacements of the O atoms. On the other hand, the protrusions forming the STM image of FeO are slightly elongated perpendicular to the direction of reconstruction as shown in Fig. 4. [This is observed for both orthogonal domains in Fig. 3(b) and therefore cannot be attributed to a tip artifact.] Therefore, it appears that an ''electronic'' factor in the formation of STM images of the FeO(111)/Pt(100) surface cannot be excluded.

The FeO(111) overlayer orientation is strongly influenced by the domain structure of the Pt substrate. Indeed, two LEED patterns in Fig. 1 show that the relative intensity of the spots coming from two orthogonal domains present on the original Pt(100)-hex surface remains the same after formation of an FeO(111)/Pt(100) coincidence structure, as indicated by the arrows. In other words, the direction of overlayer reconstruction coincides with the direction of hex reconstruction on Pt(100).

Moreover, the STM images reveal that rectangular islands are also elongated in the direction of substrate reconstruction. The islands exhibit the same surface structure as the surrounding terrace. Since we have attributed the characteristic buckling of the FeO surface to the stacking of FeO(111) layers on a Pt(100)-(1×1) square lattice, this means that the islands are in fact platinum islands covered by an FeO overlayer. Indeed, the step height of the islands of ~2 Å is the same as the atomic step height on Pt(100), both of which are imaged in Fig. 3(a). Finally, a histogram analysis of large-scale STM images show that islands cover about 30% of the entire surface, which is close to the ~25% excess of Pt atoms on the Pt(100)-hex surface relative to Pt(100)-(1×1). Therefore, we conclude that the island surface corresponds to the first FeO overlayer covering the Pt(100)-(1×1) islands that are formed by the hex$\rightarrow(1\times1)$ transformation of the Pt substrate.

Similar rectangularly shaped and elongated islands have been observed during epitaxial growth of metals on Pt(100) at temperature between 320 and 500 K for Pt,[10] and at room temperature for Au deposits.[11] At these temperatures, the surface adatoms are sufficiently mobile to produce well-defined islands. The rectangular shape of the islands is determined by the strongly anisotropic surface diffusion. Turning back to the FeO on Pt(100) system, we note that islands form only after oxidation treatment at elevated temperatures above ~700 K, but not after room-temperature Fe deposition. Therefore, we suppose that at low temperature, when the oxidation reaction proceeds slowly, platinum and iron, which are immiscible metals, behave independently. This can result in the formation of anisotropic Pt(100) islands, covered by an unoxidized iron overlayer, in a similar manner as during the hex$\rightarrow(1\times1)$ reconstruction of ''clean'' Pt(100). Another possibility is that the mass transport of the Pt adatoms occurs simultaneously with oxidation of the iron overlayer.

Thus, we find a general similarity between the growth of *metals* and of *iron oxide* on the hex-reconstructed Pt(100) surface. In all systems studied, the surface morphology is driven by a Pt substrate reconstruction, which results in formation of anisotropic islands elongated in the direction of substrate hex reconstruction.

V. SUMMARY

Well-ordered FeO monolayer films on a Pt(100)-hex substrate were grown by deposition of metallic iron and subsequent oxidation at 10^{-6} mbar of oxygen at ~750 K. Atomic-resolution STM images reveal a sine-wave height modulation of the top atomic rows along the direction of reconstruction on the original Pt(100)-hex surface. This modulation is assigned to the buckling of the top oxygen layer caused by an interaction with Pt atoms. STM images reveal the coexistence of the two superstructures described as the FeO(111)/Pt(100)-$c(2\times10)$ and (2×9) coincidence structures. It is most likely that the final structure depends on the preparation conditions and can vary with oxygen pressure and/or temperature. Nevertheless, the latter structure results in a much lower Pendry R factor in dynamical LEED analysis than reported earlier for a $c(2\times10)$ reference structure.

Numerous islands having the same surface structure as the terraces are developed on the dense FeO(111)/Pt(100) surface. They are attributed to Pt(100)-(1×1) islands underneath the FeO(111) layer, which are formed during hex $\rightarrow(1\times1)$ reconstruction of the Pt substrate. The islands are rectangular in shape and elongated in the direction of the original hex reconstruction on Pt(100). Combined STM and LEED data clearly indicate that the anisotropy in the substrate reconstruction leads to anisotropy of the oxide overlayer.

Finally, the first iron oxide layer grows on Pt(100) as a hexagonal Fe-O bilayer as on the hexagonal Pt(111)

substrate,[8] despite the mismatch of about 12% for the Pt(111) substrate and the square symmetry of the Pt(100) substrate. This indicates that the interaction within the iron oxide layer is stronger than that with the Pt substrate. It appears that the substrate-overlayer lattice mismatch does not play a dominant role in determining the overlayer structure, at least in the case of iron oxides. However, this might be not the case for other metal oxides.

*Corresponding author. FAX: (+030) 8413 4101, Email: shaikhutdinov@fhi-berlin.mpg.de

[1] G. H. Vurens, V. Maurice, M. Salmeron, and G. A. Somorjai, Surf. Sci. **268**, 170 (1992).
[2] V. Maurice, M. Salmeron, and G. A. Somorjai, Surf. Sci. **237**, 116 (1990).
[3] A. B. Boffa, H. C. Galloway, P. W. Jacobs, J. J. Benitez, J. D. Batteas, M. Salmeron, A. T. Bell, and G. A. Somorjai, Surf. Sci. **326**, 80 (1995).
[4] L. Zhang, M. Kuhn, and U. Diebold, Surf. Sci. **375**, 1 (1997).
[5] Sh. K. Shaikhutdinov, Y. Joseph, C. Kuhrs, W. Ranke, and W. Weiss, Faraday Discuss. **114**, 363 (1999).
[6] Y. J. Kim, C. Westphal, R. X. Ynzunza, H. C. Galloway, M. Salmeron, M. A. Van Hove, and C. S. Fadley, Phys. Rev. B **55**, R13 448 (1997).
[7] H. C. Galloway, J. J. Benitez, and M. Salmeron, Surf. Sci. **298**, 127 (1993).
[8] M. Ritter, W. Ranke, and W. Weiss, Phys. Rev. B **57**, 7240 (1998).
[9] M. Ritter, H. Over, and W. Weiss, Surf. Sci. **371**, 245 (1997).
[10] T. R. Linderoth, J. J. Mortensen, K. W. Jacobsen, E. Laegsgaard, I. Stensgaard, and F. Besenbacher, Phys. Rev. Lett. **77**, 87 (1996).
[11] C. Berg, H. J. Venvik, F. Strisland, and A. Borg, Surf. Sci. **409**, 1 (1998).
[12] N. Spiridis and J. Korecki, Appl. Surf. Sci. **141**, 313 (1999).
[13] W. Weiss, M. Ritter, D. Zscherpel, M. Swoboda, and R. Schlögl, J. Vac. Sci. Technol. A **16**, 21 (1998).
[14] A. Barbieri and M. A. Van Hove, SATLLEED software package.
[15] W. Weiss and M. Ritter, Phys. Rev. B **59**, 5201 (1999).
[16] A. Borg, A.-M. Hilmen, and E. Bergene, Surf. Sci. **306**, 10 (1994).
[17] S. Günter, E. Kopatzki, M. C. Bartelt, J. W. Evans, and R. J. Behm, Phys. Rev. Lett. **73**, 553 (1994).
[18] X.-C. Guo, A. Hopkinson, J. M. Bradley, and D. A. King, Surf. Sci. **278**, 263 (1992).
[19] H. C. Galloway, P. Sautet, and M. Salmeron, Phys. Rev. B **54**, R11 (1996).